

Discrimination strategies for inequivalent classes of multipartite entangled states

Sönke Niekamp,¹ Matthias Kleinmann,¹ and Otfried Gühne^{1,2}

¹*Institut für Quantenoptik und Quanteninformation,*

Österreichische Akademie der Wissenschaften, Technikerstraße 21a, A-6020 Innsbruck, Austria

²*Institut für Theoretische Physik, Universität Innsbruck, Technikerstraße 25, A-6020 Innsbruck, Austria*

(Dated: May 26, 2022)

How can one discriminate different inequivalent classes of multiparticle entanglement experimentally? We present an approach for the discrimination of an experimentally prepared state from the equivalence class of another state. We consider two possible measures for the discrimination strength of an observable. The first measure is based on the difference of expectation values, the second on the relative entropy of the probability distributions of the measurement outcomes. The interpretation of these measures and their usefulness for experiments with limited resources are discussed. In the case of graph states, the stabilizer formalism is employed to compute these quantities and to find sets of observables that result in the most decisive discrimination.

PACS numbers: 03.65.Wj, 03.67.Mn, 03.65.Ta

I. INTRODUCTION

With the rapid progress of quantum control, the experimental creation of a variety of multiparticle entangled states has become feasible [1, 2]. When more than two particles are entangled, it is well known that there are different and inequivalent entanglement classes, but there are even different classification schemes: In a first approach, one may consider two states $|\psi\rangle$ and $|\phi\rangle$ as equivalent, if one can be converted into the other by changing the local bases only. These operations are called local unitary (LU) operations and recently a method to decide whether two states are LU equivalent or not has been found [3, 4]. Another classification is based on the question regarding whether a single copy of $|\psi\rangle$ can be converted into $|\phi\rangle$ by local operations and classical communication, even if this conversion works only with a small probability [5]. These operations are called stochastic local operations and classical communication (SLOCC). Similar to LU equivalent states, states equivalent under SLOCC can often be used for the same applications. As the number of SLOCC classes is infinite for more than three qubits [6], modified classification schemes have been proposed [7, 8].

On the theoretical side, it has been shown that different classes of entangled states are suited for different applications. For example, cluster states are useful for one-way quantum computation, whereas Greenberger-Horne-Zeilinger (GHZ) states are not [9]. To the contrary, for sub shot-noise interferometry, GHZ states are optimally suited, while cluster states are useless for this task [10]. Consequently, it can be important to discriminate experimentally between the different classes.

For the experimental verification of entanglement, a number of tools exist—the most prominent example are witness operators [11]. As experiments no longer aim only at the creation of entanglement but also at creating specific classes of entangled states, tools are needed for the experimental discrimination of these classes. In the context of entanglement detection, it is well known that a

given Bell inequality or witness operator detects only a part of all entangled states and fails to detect others. Thus the violation (or nonviolation) of a Bell inequality can provide information not only about the entanglement present in a state but also about its type [12, 13].

Consequently, in Ref. [14] Bell operators have been constructed and experimentally implemented for discriminating different classes of entangled states. For an experiment aiming at the creation of a particular state, a Bell operator characteristic for this state was designed, that is, a Bell operator that has the desired state as eigenstate with maximal eigenvalue. The maximal expectation value of this Bell operator for various other classes of states (defined as all LU equivalents or all SLOCC equivalents of some prominent entangled state) was determined. Measuring the Bell operator then proved that the prepared state was not in those classes with maximal expectation value lower than the experimentally obtained value. In this approach, the characteristic operator is far from unique. Neither is it necessary to use a Bell operator, as has already been remarked in Ref. [14]. As entangled states with increasingly large numbers of qubits are being prepared, analysis tools that give strong results in spite of a limited number of measurement events are needed. In the context of entanglement detection this problem has recently received attention [15–17].

In this article we present an approach for the discrimination of an experimentally prepared state from the class of all local unitaries of another state. We define two measures for the discrimination strength of an observable. The first measure is based on the difference of expectation values and coincides with the one implicitly used in Ref. [14]. An interpretation of this quantity as a noise tolerance is presented. The second measure is based on the relative entropy, also called Kullback-Leibler divergence, which is a well-established information-theoretic measure for the discrepancy of two classical probability distributions [18, 19]. This quantity is directly related to the probability of another state to reproduce the observed measurement outcomes in a given number of measure-

ment runs. Our use of the relative entropy is motivated by a work of van Dam *et al.*, where it was used to assess the statistical strength of nonlocality proofs [15]. In the case of graph states, the stabilizer formalism helps us to compute these quantities and to find sets of observables that result in the strongest discrimination. We would like to add that our approach is not directly related to the task of state discrimination as it is often discussed in the literature [20]. In particular we do not assume the promise that the state is either in the first or in the second family; such an assumption cannot be justified in an experiment aiming for the verification of entanglement properties.

This article is organized as follows: In Section II we introduce the two measures for the discrimination strength. In Sections III and IV we calculate these quantities for certain four- and three-qubit states and find optimal sets of observables for the discrimination task. The performance of the measures for experimental data and noisy states is investigated. In Section V a general result for the discrimination of graph states is presented. Finally, Section VI is devoted to a discussion of the results.

II. THE SITUATION AND THE DISTANCE MEASURES

We consider the following situation: In an experiment aiming at the preparation of a state ϱ the experimenter wants to verify that the prepared state is not in a certain class of undesired states, given by all local unitaries (and maybe permutations of qubits) of a pure state $|\phi\rangle$. For that, he can measure an observable A (or several observables A_i) and one has to define to what extent such a measurement can exclude the undesired states.

In this section we will define two quantities that measure how well an observable A discriminates a state ϱ from all local unitaries of another state $|\phi\rangle$. While we are restricting our attention to LU classes in this article, it should be noted that the same quantities can also be defined for SLOCC classes.

A. A measure based on the fidelity

In analogy to the approach taken in Ref. [14] we define the fidelity based measure as

$$\mathcal{F}_A(\varrho||\phi) = \min_{U \in \text{LU}} |\text{Tr}(A\varrho) - \langle \phi|U^\dagger A U|\phi \rangle|. \quad (1)$$

Here the minimization is over all local unitaries U ; later we will consider also the minimization over all permutations of qubits.

Adding or subtracting a multiple of the identity matrix to A does not change the value of \mathcal{F} in Eq. (1). So without loss of generality we can assume $\text{Tr}(A) = 0$. Also without loss of generality we assume $\text{Tr}(A\varrho) \geq 0$.

In the following we will always assume that $\text{Tr}(A\varrho) \geq \max_{\text{LU}} \langle \phi|A|\phi \rangle$. This is no restriction for our purposes

due to the following reasoning: Let us assume that for the pure n -qubit state $|\phi\rangle$ there exist 2^n local unitaries U_i such that $\{U_i|\phi\rangle\}$ forms an orthonormal basis. States with this property are called locally encodeable [21]. It has been conjectured that all pure states are locally encodeable, and the conjecture has been proven for a variety of states, including all stabilizer states and the W state [21]. Then we can write $\mathbb{1} = \sum_i U_i|\phi\rangle\langle\phi|U_i^\dagger$ and since A is traceless we have $\text{Tr}(A \sum_i U_i|\phi\rangle\langle\phi|U_i^\dagger) = 0$. So, if $\langle \phi|A|\phi \rangle < 0$ there exists a local unitary U such that $\langle \phi|U^\dagger A U|\phi \rangle > 0$ and vice versa. If $\max_{\text{LU}} \langle \phi|A|\phi \rangle \geq \text{Tr}(A\varrho)$, by local encodeability there exists a local unitary U such that $\text{Tr}(A\varrho) \geq 0 \geq \langle \phi|U^\dagger A U|\phi \rangle$. By continuity there exists another local unitary such that $\text{Tr}(A\varrho) = \langle \phi|U^\dagger A U|\phi \rangle$, i. e., $\mathcal{F}_A(\varrho||\phi) = 0$ and the observable A is not suitable for a discrimination procedure based on \mathcal{F} . In this article, we shall be concerned with graph states and sometimes with the W state, so local encodeability is proven for our purposes and we have

$$\mathcal{F}_A(\varrho||\phi) = \text{Tr}(A\varrho) - \max_{\text{LU}} \langle \phi|A|\phi \rangle. \quad (2)$$

This quantity, however, is not invariant under rescaling of A . To be able to compare different observables, we have to agree on a normalization. We choose $\text{Tr}(A\varrho) = 1$, which is the same normalization as in Ref. [14], and obtain

$$\mathcal{F}_A(\varrho||\phi) = 1 - \max_{\text{LU}} \langle \phi|A|\phi \rangle. \quad (3)$$

This is the first quantity that will serve us as a measure for the strength with which A discriminates ϱ from all local unitaries of $|\phi\rangle$.

For more than one observable we define

$$\mathcal{F}_{A_1, \dots, A_k}(\varrho||\phi) = \mathcal{F}_{\frac{1}{k} \sum_{i=1}^k A_i}(\varrho||\phi). \quad (4)$$

In the remainder of the article we will discuss how to find optimal families of observables A_1, \dots, A_k for particular states ϱ and $|\phi\rangle$.

Our definition has a direct physical interpretation in terms of a noise tolerance. For that, we exploit the similarity of our problem to the task of entanglement detection by virtue of witness operators and consider the robustness of \mathcal{F} in Eq. (2) against white noise: Let

$$\varrho_{\text{wn}}(p) = (1-p) \frac{\mathbb{1}}{d} + p\varrho \quad (5)$$

be the state ϱ affected by white noise. The maximal noise level $(1-p)$ such that

$$\text{Tr}[A\varrho_{\text{wn}}(p)] - \max_{\text{LU}} \langle \phi|A|\phi \rangle \geq 0 \quad (6)$$

is given by [using $\text{Tr}(A) = 0$]

$$1-p = 1 - \max_{\text{LU}} \langle \phi|A|\phi \rangle = \mathcal{F}_A(\varrho||\phi). \quad (7)$$

We will discuss the interpretation of \mathcal{F} as a noise tolerance in more detail in Section III C.

B. A measure based on the relative entropy

From a statistical point of view, the task of discriminating a state ϱ and a state $\sigma = |\phi\rangle\langle\phi|$ by virtue of an observable A is the task of discriminating the corresponding probability distributions for the measurement outcomes of A .

The relative entropy or Kullback-Leibler divergence is a well-established information-theoretic measure for the discrepancy between two classical probability distributions [18, 19]. The relative entropy of the probability distributions $P = \{p_1, \dots, p_m\}$ and $Q = \{q_1, \dots, q_m\}$ is defined as

$$D(P\|Q) = \sum_{i=1}^m p_i \log\left(\frac{p_i}{q_i}\right). \quad (8)$$

We will always use the logarithm to the base of two, $\log = \log_2$, and define $0 \log(0) = 0$. Note that since we are dealing with the discrimination of classical probability distributions, we are not using the quantum (or von Neumann) relative entropy [19], $\text{Tr}[\varrho(\log \varrho - \log \sigma)]$. The relative entropy satisfies $0 \leq D(P\|Q) \leq \infty$ with $D(P\|Q) = 0$ if and only if $P = Q$. But although the relative entropy behaves in some sense like a distance between probability distributions, it is not a metric because it is not symmetric. The most important properties of the relative entropy are summarized in Appendix A.

Concerning the interpretation, the relative entropy $D(P\|Q)$ can be used to answer the question: How strongly does a sample (of a fixed length) from the distribution P on average indicate that it was indeed drawn from P rather than from Q ? This statement can be made precise with the theory of statistical hypothesis testing [15].

For the simplest case, note that $D(P\|Q)$ is infinity if and only if $q_i = 0$, but $p_i > 0$ for some i , that is, if an event is impossible according to Q , but occurs with a nonvanishing probability according to P . This means that on observing this event one immediately knows that the sample was not drawn from Q .

More generally, suppose that a sample of length N has been drawn from Q . We consider the empirical probability distribution P defined by the observed frequencies. Then the probability $Q^N[T(P)]$ of drawing a sample from Q with the same frequencies [i. e., within the type class $T(P)$] decays exponentially for large N [18, Thm. 12.1.4],

$$Q^N[T(P)] \sim 2^{-ND(P\|Q)}. \quad (9)$$

Consequently, if one observes a probability distribution P yielding a large value for the relative entropy $D(P\|Q)$, the assumption that it was rather drawn from the probability distribution Q is very questionable (see also below).

Let us now return to our original problem: For an experiment aiming at the preparation of the state ϱ , we define a measure for how well the observable A can exclude the state σ as the relative entropy of the corresponding

measurement outcomes for A

$$D_A(\varrho\|\sigma) = \sum_{i=1}^m \text{Tr}(\varrho\Pi_i) \log\left(\frac{\text{Tr}(\varrho\Pi_i)}{\text{Tr}(\sigma\Pi_i)}\right), \quad (10)$$

where $A = \sum_{i=1}^m a_i\Pi_i$ is the spectral decomposition of A . From the above discussion, this is a measure for how strongly the measurement results of the observable A on the state ϱ on average show that they are due to the state ϱ rather than the state σ . (Note, that in this interpretation we assume that the experimental precision in implementing the observable A outperforms the precision that can be achieved for the preparation of the state ϱ .)

Let us discuss the interpretation of this quantity. Suppose that the measurement has been performed, resulting in an observed probability distribution $\tilde{P} = \{\tilde{p}_1, \dots, \tilde{p}_m\}$ of the outcomes a_1, \dots, a_m , and let \tilde{N} be the number of measurement runs. Then, by Eq. (9), the probability that a measurement on the state σ , after \tilde{N} measurement runs, results in the same frequencies is given by

$$Q^{\tilde{N}}[T(\tilde{P})] \sim 2^{-\tilde{N}D(\tilde{P}\|Q)}, \quad (11)$$

where $Q = \{\text{Tr}(\sigma\Pi_1), \dots, \text{Tr}(\sigma\Pi_m)\}$. If the experimentally prepared state is close enough to the intended state ϱ , the relative entropy $D(\tilde{P}\|Q)$ will attain a large value only if this is already the case for $D_A(\varrho\|\sigma)$.

For comparison, when tossing a fair coin N times, the probability of the outcome always being “tails” is

$$2^{-ND(\{1,0\}\|\{\frac{1}{2},\frac{1}{2}\})} = 2^{-N} \quad (12)$$

since Eq. (9) is exact in this example. Thus, the probability Eq. (11) of obtaining the frequencies \tilde{P} after measuring \tilde{N} times the state σ is equal to the probability of always obtaining “tails” in $N = \tilde{N}D(\tilde{P}\|Q)$ tosses of a fair coin [15]. In other words, the likelihood after \tilde{N} measurement runs that the prepared state is σ is the same as that of a coin to be fair after $N = \tilde{N}D(\tilde{P}\|Q)$ tosses resulting in “tails”. This gives our results for the measure D in Eq. (10) a quantitative interpretation.

When measuring several observables A_1, \dots, A_k independently of each other, the relative entropy of the joint probability distributions is given by the sum of the relative entropies for the individual observables (cf. Property 5 in Appendix A). However, we renormalize the relative entropy in this case and define

$$D_{A_1, \dots, A_k}(\varrho\|\sigma) = \frac{1}{k} \sum_{i=1}^k D_{A_i}(\varrho\|\sigma), \quad (13)$$

where the prefactor $1/k$ corresponds to keeping the overall number of measurement runs constant, independent of the number of observables, i. e., each observable A_i will be measured in \tilde{N}/k runs. We choose this definition because in experiments the rate at which entangled states are being created is typically low, so the number of measurement runs is a scarce resource.

Finally, we consider the minimum of D over all local unitaries of σ ,

$$\mathcal{D}_{A_1, \dots, A_k}(\varrho \|\sigma) = \min_{U \in \text{LU}} D_{A_1, \dots, A_k}(\varrho \| U\sigma U^\dagger). \quad (14)$$

In the following we will discuss how to find families of observables A_i which maximize this quantity.

III. DISCRIMINATING FOUR-QUBIT STATES

As our first example, we will calculate the quantities \mathcal{F} and \mathcal{D} for the discrimination of the four-qubit GHZ state from the four-qubit linear cluster state and vice versa.

The four-qubit GHZ state is given by

$$|\text{GHZ}_4\rangle = \frac{1}{\sqrt{2}}(|0000\rangle + |1111\rangle). \quad (15)$$

Alternatively, it can be described by its stabilizing operators: The GHZ state is the unique common eigenstate with eigenvalue +1 of the 16 operators

$$S_{\text{GHZ}_4} = \{\mathbb{1}\mathbb{1}\mathbb{1}\mathbb{1}, \mathbb{1}\mathbb{1}ZZ \text{ and perm.}, ZZZZ, \\ XXXX, -XXYY \text{ and perm.}, YYYYY\}. \quad (16)$$

Here and in the following X , Y , Z , and $\mathbb{1}$ denote the Pauli matrices and the identity, tensor product signs have been omitted and ‘‘perm’’ denotes all possible permutations of the qubits which give different terms. The set of all stabilizing operators forms a commutative group, and the GHZ state is an example of a graph state [22]. We will explain this in more detail in Section V below. The sum of all stabilizing operators gives the projector onto the state

$$|\text{GHZ}_4\rangle\langle\text{GHZ}_4| = \frac{1}{16} \sum_{S \in S_{\text{GHZ}_4}} S, \quad (17)$$

this property is shared by any graph state. The stabilizing operators thus contain a description of the correlations present in the state.

The linear cluster state given by

$$|C_4\rangle = \frac{1}{2}(|0000\rangle + |0011\rangle + |1100\rangle - |1111\rangle) \quad (18)$$

is also a graph state: Its stabilizer group is [22]

$$S_{C_4} = \{\mathbb{1}\mathbb{1}\mathbb{1}\mathbb{1}, \mathbb{1}\mathbb{1}ZZ, ZZ\mathbb{1}\mathbb{1}, ZZZZ, \\ XYXY, XYYX, YXXY, YXYX, \\ \mathbb{1}ZXX, Z\mathbb{1}XX, XX\mathbb{1}Z, XXZ\mathbb{1}, \\ -\mathbb{1}ZYY, -Z\mathbb{1}YY, -YY\mathbb{1}Z, -YYZ\mathbb{1}\}, \quad (19)$$

and the analogous relation to Eq. (17) holds.

The stabilizing operators of a graph state $|\psi\rangle$ provide a natural choice of observables for the discrimination of $\varrho = |\psi\rangle\langle\psi|$ from other states. In the language of Ref. [14], they are characteristic operators for the graph state. In the following we will restrict our analysis to these observables.

A. Discriminating the GHZ state from the cluster state

We first consider the discrimination of the GHZ state from all LU equivalents of the cluster state, using all stabilizing operators of the former, excluding only the identity, as it is useless for any discrimination task. We introduce the notation $S^* = S \setminus \{\mathbb{1}\}$ for any stabilizer group S minus the identity. Later we will discuss which *subset* of the stabilizer group gives the strongest discrimination. We start with the calculation of the quantity \mathcal{D} in Eq. (14), which is based on the relative entropy.

It is useful to think of the cluster state as the sum of its stabilizing operators $|C_4\rangle\langle C_4| = \frac{1}{16} \sum_{T \in S_{C_4}} T$. For any GHZ stabilizing operator $S \in S_{\text{GHZ}_4}^*$, the term D_S is a function of the overlap of S with the stabilizing operators of the cluster state

$$D_S(\text{GHZ}_4 \| C_4) = -\log \left\{ \frac{1}{2} \left[\frac{1}{16} \sum_{T \in S_C} \text{Tr}(ST) + 1 \right] \right\}. \quad (20)$$

If we do not consider local unitaries, $\text{Tr}(ST)$ is zero unless $S = T$. For the minimization over local unitaries in Eq. (14) we classify stabilizing operators by the qubits on which they act nontrivially. For any GHZ stabilizing operator S , only those stabilizing operators of $|C_4\rangle$ which act nontrivially on the exactly the same qubits as S can have a nonvanishing overlap with S . This still holds if arbitrary local unitary operations are applied to $|C_4\rangle$. We can thus identify those stabilizing operators of $|C_4\rangle$ that can contribute to D_S .

If no local unitary is applied, the GHZ stabilizing operators $\mathbb{1}\mathbb{1}ZZ$, $ZZ\mathbb{1}\mathbb{1}$, and $ZZZZ$ have maximal overlap with cluster stabilizing operators and thus give the minimal relative entropy of zero, while $\mathbb{1}Z\mathbb{1}Z$, $\mathbb{1}ZZ\mathbb{1}$, $Z\mathbb{1}\mathbb{1}Z$, and $Z\mathbb{1}Z\mathbb{1}$ each have zero overlap and thus give relative entropy of 1. A minimization over local unitaries cannot improve this result, as the cluster state has no stabilizing operators acting nontrivially on the same qubits.

All of the remaining stabilizing operators of $|\text{GHZ}_4\rangle$

$$\Sigma = \{XXXX, -XXYY, -YYXX, YYYY, \\ -XYXY, -XYYX, -YXXY, -YXYX\} \quad (21)$$

act on all four qubits (such stabilizing operators describing four-point correlations we call four-point stabilizing operators for short). We note that both these and the four-point stabilizing operators of $|C_4\rangle$ except $ZZZZ$ are products of local operators X and Y . It is therefore reasonable to assume that for the minimization of D_Σ it suffices to consider rotations about the z axes. The rotated cluster state is

$$|C_4(\gamma, \delta)\rangle = \frac{1}{2}(|0000\rangle + e^{-i\delta}|0011\rangle \\ + e^{-i\gamma}|1100\rangle - e^{-i(\gamma+\delta)}|1111\rangle), \quad (22)$$

where $\gamma = \varphi_1 + \varphi_2$, $\delta = \varphi_3 + \varphi_4$, and the φ_i are the rotation angles about the local z axes, and we obtain $D_{\Sigma}(\text{GHZ}_4 \| C_4(\gamma, \delta)) = -\frac{1}{2} \left[\log \left[\frac{1}{2} (1 + \sin(\gamma) \sin(\delta)) \right] \right] +$

$\log[\frac{1}{2}(1 - \cos(\gamma)\cos(\delta))]$. The minimum of this expression is $-\log(3/4)$. In conclusion, we have found that

$$\mathcal{D}_{S_{\text{GHZ}_4}^*}(\text{GHZ}_4\|C_4) = \frac{1}{15}(4 - 8\log\frac{3}{4}) \approx 0.4880. \quad (23)$$

Since our analytic optimization required an assumption we would like to add that this result is also obtained via numerical minimization over all local unitaries. The 15 GHZ stabilizing operators do not contribute equally to \mathcal{D} , rather, $D = 0$ for $\mathbb{1}\mathbb{1}ZZ$, $ZZ\mathbb{1}\mathbb{1}$, and $ZZZZ$; $D = 1$ for $\mathbb{1}Z\mathbb{1}Z$, $\mathbb{1}ZZ\mathbb{1}$, $Z\mathbb{1}\mathbb{1}Z$, and $Z\mathbb{1}Z\mathbb{1}$; and $D = -\log(3/4) \approx 0.4150$ for all others.

Let us now turn to the fidelity-based measure \mathcal{F} for the same observables and states. If we use all stabilizing operators of $|\psi\rangle$, excluding again only the identity, $\mathcal{F}(\psi\|\phi)$ is a function of the fidelity

$$\mathcal{F}_{S_{\psi}^*}(\psi\|\phi) = \frac{2^n}{2^n - 1} \left(1 - \max_{\text{LU}} |\langle\psi|\phi\rangle|^2\right), \quad (24)$$

where n is the number of qubits.

For our example, we note that for an arbitrary local unitary U we have $|\langle\text{GHZ}_4|U|C_4\rangle|^2 \leq 1/2$ and this bound can be reached. This follows from the known fact that the maximal overlap of the cluster state with any product state, and thus with $|0000\rangle$ and $|1111\rangle$, is given by $1/4$ [23] and one can easily find a local unitary with $|\langle\text{GHZ}_4|U|C_4\rangle|^2 = 1/2$. So we have

$$\mathcal{F}_{S_{\text{GHZ}_4}^*}(\text{GHZ}_4\|C_4) = \frac{8}{15} \quad (25)$$

as the fidelity-based measure for the discrimination.

Let us now discuss subsets of the stabilizer group as observables for the discrimination. In our previous analysis, it turned out that not all stabilizing operators contribute equally to the discrimination, in fact, some of them do not contribute at all. We therefore ask for families of stabilizing operators of $|\text{GHZ}_4\rangle$ that discriminate $|\text{GHZ}_4\rangle$ from the local unitaries of $|C_4\rangle$ most strongly, that is, families for which \mathcal{F} (or \mathcal{D}) is maximal.

From the previous discussion, candidates are

$$\mathbb{1}Z\mathbb{1}Z, \mathbb{1}ZZ\mathbb{1}, Z\mathbb{1}\mathbb{1}Z, Z\mathbb{1}Z\mathbb{1}, \quad (26)$$

since any of them gives $\mathcal{F} = \mathcal{D} = 1$. But if we want to exclude not only all LU equivalents, but also all permutations of qubits of the cluster state, we still have to minimize \mathcal{F} and \mathcal{D} over all permutations, because the set of observables is no longer necessarily permutation invariant. There are three distinct permutations of the cluster state, namely $|C^1\rangle = |C_4\rangle = \frac{1}{2}(|0000\rangle + |0011\rangle + |1100\rangle - |1111\rangle)$, $|C^2\rangle = \frac{1}{2}(|0000\rangle + |0110\rangle + |1001\rangle - |1111\rangle)$, and $|C^3\rangle = \frac{1}{2}(|0000\rangle + |0101\rangle + |1010\rangle - |1111\rangle)$. Table I shows the GHZ stabilizing operators from Eq. (26) along with all stabilizing operators of the permutations of $|C_4\rangle$ that act on the same qubits. We see that any single one of these six stabilizing operators gives a relative entropy of zero, if the entropy is minimized over all

$ \text{GHZ}_4\rangle$	$ C^1\rangle$	$ C^2\rangle$	$ C^3\rangle$
$\mathbb{1}\mathbb{1}ZZ$	$\mathbb{1}\mathbb{1}ZZ$		
$\mathbb{1}Z\mathbb{1}Z$			$\mathbb{1}Z\mathbb{1}Z$
$\mathbb{1}ZZ\mathbb{1}$		$\mathbb{1}ZZ\mathbb{1}$	
$Z\mathbb{1}\mathbb{1}Z$		$Z\mathbb{1}\mathbb{1}Z$	
$Z\mathbb{1}Z\mathbb{1}$			$Z\mathbb{1}Z\mathbb{1}$
$ZZ\mathbb{1}\mathbb{1}$	$ZZ\mathbb{1}\mathbb{1}$		

TABLE I: Stabilizing operators of the GHZ state and stabilizing operators of the three permutations of the cluster state acting on the same qubits (see text for further details).

permutations. Any pair of stabilizing operators gives an entropy of either zero or $1/2$. The three-element family $\{\mathbb{1}\mathbb{1}ZZ, \mathbb{1}Z\mathbb{1}Z, \mathbb{1}ZZ\mathbb{1}\}$ gives $2/3$, in total there are eight such families giving the same value.

It is easy to see that these families of stabilizing operators are optimal: It is clear that they are optimal among all subsets of the six stabilizing operators in the table. Furthermore, we recall that we found a local unitary transformation such that all remaining stabilizing operators contribute either 0 or $-\log(3/4)$ to the entropy. Because of the permutation invariance of the set of these remaining stabilizing operators, this holds for all permutations of $|C_4\rangle$. As $-\log(3/4) < 2/3$, adding some of the remaining observables cannot improve the discrimination. This shows the optimality of our three-element families. These families are also optimal when using \mathcal{F} instead of \mathcal{D} .

We summarize the main results of this subsection in the following observation:

Observation. *For the discrimination of the GHZ state from all local unitaries and permutations of qubits of the cluster state, using all GHZ stabilizing operators except the identity, the measures \mathcal{D} and \mathcal{F} are given by Eqs. (23) and (25). When considering subsets of the stabilizer group, $\{\mathbb{1}\mathbb{1}ZZ, \mathbb{1}Z\mathbb{1}Z, \mathbb{1}ZZ\mathbb{1}\}$ is an example of an optimal family of observables, giving $\mathcal{F} = \mathcal{D} = 2/3$.*

Finally, let us add that until now we assumed that all observables are measured independently. However, as the observables in Eq. (26), from which we constructed the optimal families, have a common eigenbasis of product states (the computational basis), they can also be measured jointly in one experiment with more than two outcomes. In this case, the relative entropy is no longer given by Eq. (13). When measuring the computational basis in one experiment with 16 outcomes, we obtain

$$\begin{aligned} \mathcal{D} &= \min_{U \in \text{LU}} \sum_{i=1}^{16} |\langle e_i | \text{GHZ}_4 \rangle|^2 \log \left(\frac{|\langle e_i | \text{GHZ}_4 \rangle|^2}{|\langle e_i | U | C_4 \rangle|^2} \right) \\ &= 1. \end{aligned} \quad (27)$$

Consequently, considering measurements with more outcomes can give a stronger discrimination. This is a consequence of a general feature of the relative entropy: For

each of the observables in Eq. (26), the probability distribution for the measurement outcomes is obtained from the one for the measurement of the computational basis by considering several events as one (in other words, by “forgetting” information). The relative entropy satisfies a grouping rule similar to the Shannon entropy (Property 4 in Appendix A), which implies that this process can only decrease the relative entropy.

B. Discriminating the cluster state from the GHZ state

Let us now consider the reverse discrimination $\mathcal{D}_{S_{C_4}^*}(C_4\|\text{GHZ}_4)$. This turns out to be relatively simple.

First, note that the eight three-point stabilizing operators of $|C_4\rangle$ will for any local unitary operation have zero overlap with $|\text{GHZ}_4\rangle$ as the GHZ state has no three-point stabilizing operators. For the remaining eight stabilizing operators, however, the overlap with the GHZ state can be brought to 1 by an appropriate rotation, as one can directly check. Thus

$$\mathcal{D}_{S_{C_4}^*}(C_4\|\text{GHZ}_4) = \frac{8}{15}. \quad (28)$$

As a function of the fidelity, \mathcal{F} is the same as for the reverse discrimination

$$\mathcal{F}_{S_{C_4}^*}(C_4\|\text{GHZ}_4) = \frac{8}{15}. \quad (29)$$

Considering the optimal subsets of the stabilizer group, it is clear that any set of three-point stabilizing operators of $|C_4\rangle$ is an optimal family of observables, resulting in $\mathcal{D} = \mathcal{F} = 1$. Note that the GHZ state is permutation invariant, so the optimization over permutations does not play a role.

C. Application to a four-photon experiment

To study the noise tolerance of the quantities \mathcal{F} and \mathcal{D} and their performance for experimental data, we use the measurement results for the stabilizer correlations of the cluster state obtained by Kiesel *et al.* in a photonic experiment [13]. When using all cluster stabilizing operators for the discrimination (excluding the identity), these data give

$$\mathcal{F}_{S_{C_4}^*}(\varrho_{\text{exp}}\|\text{GHZ}_4) = 0.257 \pm 0.014, \quad (30)$$

$$\mathcal{D}_{S_{C_4}^*}(\varrho_{\text{exp}}\|\text{GHZ}_4) = 0.189 \pm 0.012. \quad (31)$$

When using only the three-point stabilizing operators, which form an optimal family Q , we get

$$\mathcal{F}_Q(\varrho_{\text{exp}}\|\text{GHZ}_4) = 0.668 \pm 0.019, \quad (32)$$

$$\mathcal{D}_Q(\varrho_{\text{exp}}\|\text{GHZ}_4) = 0.353 \pm 0.021. \quad (33)$$

Note that in all cases the observables are normalized with respect to the perfect cluster state as $\langle C_4|A_i|C_4\rangle = 1$, while for the experimental data we have $\text{Tr}(\varrho_{\text{exp}}A_i) < 1$. Also, it should be noted that the subsets of observables we use were chosen to be optimal for the perfect cluster state but not necessarily for the experimental one. This, however, is similar to the implementation of entanglement witnesses in experiments: There, one typically considers some optimal witness for some pure state that one aims to prepare and applies it to the experimental data in order to obtain a significant entanglement test [11].

To investigate the power of our discrimination methods, we calculate \mathcal{F} and \mathcal{D} for both the perfect and the experimental cluster state under the influence of white noise. Figures 1 and 2 show \mathcal{F} and \mathcal{D} as functions of the noise level. We make a number of observations:

For the perfect cluster state with additional white noise, the quantity \mathcal{F} decreases with increasing noise level until it reaches zero at the noise level $(1 - p) = \mathcal{F}(C_4\|\text{GHZ}_4)$. This interpretation of \mathcal{F} as a noise tolerance was already mentioned in Section II A. Note, however, that in the case of the experimental state the noise tolerance is no longer given by $\mathcal{F}(\varrho_{\text{exp}}\|\text{GHZ}_4)$ but is larger due to $\text{Tr}(\varrho_{\text{exp}}A_i) < 1$.

For the same observables, the maximal noise level at which $\mathcal{D} > 0$ is at least as high as the maximal noise level at which $\mathcal{F} > 0$. This is a general feature: As a consequence of the positive definiteness of the relative entropy, \mathcal{D} is nonzero whenever \mathcal{F} is. In this particular example, \mathcal{D} is nonzero for noise levels arbitrarily close to 1, though this is not a general feature.

For the three-point stabilizing operators of $|C_4\rangle$, also the noise tolerance of \mathcal{F} is 1 (Fig. 2). It is instructive to compare this to the case of witness operators: The set of separable states contains a ball around the completely mixed state [24], which implies that for any witness W and entangled state ϱ detected by W the noise tolerance is strictly less than 1. In our case the situation is different: The reason for the noise tolerance of one is that no local unitaries of the GHZ state have any three-point correlations. This implies that the set of states LU equivalent to $|\text{GHZ}_4\rangle$ does not contain a ball around $\mathbb{1}/d$. For a fair comparison, one may therefore consider the three-point correlations in experiments *aiming* at the generation of GHZ states (for instance, in Ref. [25] they were maximally 0.097) and ask whether the measured three-point stabilizer correlations in a cluster state experiment significantly exceed these values.

Comparing the figures shows another difference between the measures \mathcal{F} and \mathcal{D} : For the measure \mathcal{F} , the noise tolerance is higher in the case of the three-point stabilizing operators (Fig. 2) than in the case of all stabilizing operators (Fig. 1). This is remarkable because the former set of observables is contained in the latter. In other words, adding an observable can reduce the noise tolerance of \mathcal{F} . From the definition of the quantity \mathcal{D} it is clear that its noise tolerance of $\mathcal{D}_{A_1, \dots, A_k}$ is lower bounded by the noise tolerance of \mathcal{D} for any subset of

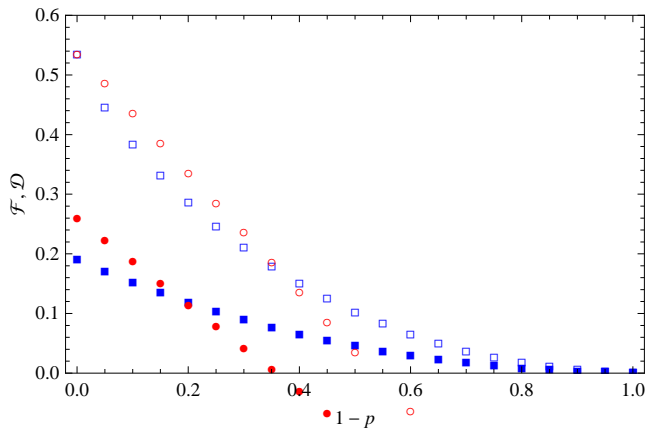


FIG. 1: Discriminating the four-qubit linear cluster state with noise from all local unitaries of the GHZ state, using all stabilizing operators of the former. Shown are \mathcal{F} (red circles) and \mathcal{D} (blue squares) versus the level of white noise ($1-p$) for the perfect (empty symbols) and the experimental (filled symbols) state.

A_1, \dots, A_k . In Ref. [26], a quantity similar to \mathcal{F} was constructed from the correlations of an entangled state and used for entanglement detection. The same phenomenon of a decreasing noise tolerance when including more correlations was observed.

The preceding observations concerning the comparison of the measures \mathcal{F} and \mathcal{D} can be understood by noting that the relative entropy uses all information contained in the probability distributions for the measurement outcomes, whereas the quantity \mathcal{F} effectively reduces each probability distribution to one parameter.

We recall that the value of the relative entropy \mathcal{D} has an interpretation in terms of probabilities (Section II B). This is in contrast to the quantity \mathcal{F} , whose numerical value is fixed only by a normalization condition on the observables (Section II A). While in certain cases it can be interpreted as a noise tolerance and it is useful for comparing different observables, it gives no quantitative statement about the discrepancy between the prepared state and states which we want to exclude. Finally, we note that in experimental applications also the error estimates for either quantity must be taken into account. Though we have done so in Eqs. (30)–(33), a systematic analysis of this point is beyond the scope of our present article.

IV. DISCRIMINATING THREE-QUBIT STATES

Now we consider the three-qubit case, aiming at the discrimination of the three-qubit GHZ state and the three-qubit W state. These two states are relevant as representatives of the two different entanglement classes of genuine three-qubit entanglement [5].

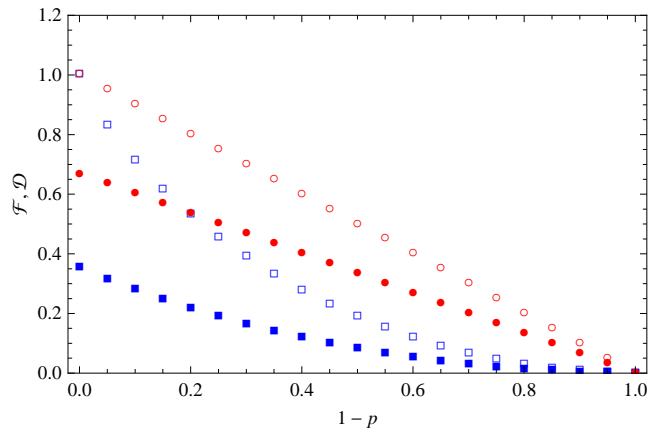


FIG. 2: Discriminating the four-qubit linear cluster state with noise from all local unitaries of the GHZ state, using all three-point stabilizing operators of the former. Symbols as in Fig. 1.

The three-qubit GHZ state is given by

$$|\text{GHZ}_3\rangle = \frac{1}{\sqrt{2}}(|000\rangle + |111\rangle). \quad (34)$$

As in the four-qubit case, this state can be described by its stabilizing operators. The stabilizer group is given by the eight observables

$$S_{\text{GHZ}_3} = \{\mathbb{1}\mathbb{1}\mathbb{1}, \mathbb{1}ZZ \text{ and perm.}, \\ XXX, -XYY \text{ and perm.}\}. \quad (35)$$

The three-qubit W state

$$|\text{W}_3\rangle = \frac{1}{\sqrt{3}}(|001\rangle + |010\rangle + |100\rangle) \quad (36)$$

is not a stabilizer state. If we expand its density matrix into Pauli matrices we arrive at

$$|\text{W}_3\rangle\langle\text{W}_3| = \frac{1}{24} [3 \cdot \mathbb{1}\mathbb{1}\mathbb{1} + (\mathbb{1}\mathbb{1}Z + \text{perm.}) \\ + 2(\mathbb{1}XX + \text{perm.}) + 2(\mathbb{1}YY + \text{perm.}) - (\mathbb{1}ZZ + \text{perm.}) \\ + 2(XXZ + \text{perm.}) + 2(YYZ + \text{perm.}) - 3 \cdot ZZZ]. \quad (37)$$

A. Discriminating the GHZ state from the W state

Again, we will first compute \mathcal{F} and \mathcal{D} for the case that all stabilizing operators (except for $\mathbb{1}$) of the GHZ state are used, and afterwards look for optimal families of observables.

Parameterizing local unitaries as $U(\varphi, \theta, \psi) = \exp(i\psi\sigma_z/2) \exp(i\theta\sigma_y/2) \exp(i\varphi\sigma_z/2)$, we obtain $\langle\text{W}_3|U^\dagger \mathbb{1}ZZ U|\text{W}_3\rangle = \frac{1}{3}[-\cos(\theta_2)\cos(\theta_3) + 2\cos(\varphi_2 - \varphi_3)\sin(\theta_2)\sin(\theta_3)]$. The expectation values of $Z\mathbb{1}Z$ and $ZZ\mathbb{1}$ can be obtained by cyclically permuting the indices of the angles, as the W state is permutationally invariant.

We find $\max_{LU} \langle W_3 | \mathbb{1}ZZ | W_3 \rangle = 2/3$, where the maximum is attained when $\cos(\varphi_2 - \varphi_3) \sin(\theta_2) \sin(\theta_3) = 1$. Thus the expectation values of $\mathbb{1}ZZ$, $Z\mathbb{1}Z$, and $ZZ\mathbb{1}$ can be maximized simultaneously. We choose the solution $\varphi_1 = \varphi_2 = \varphi_3 = 0$ and $\theta_1 = \theta_2 = \theta_3 = \pi/2$.

Let us now consider the remaining stabilizing operators. Assuming the above choice for the angles φ_i and θ_i and making the symmetry assumption $\psi_1 = \psi_2 = \psi_3 = \psi$, we have $\langle W_3 | U^\dagger XXXU | W_3 \rangle = 3 \cos^3(\psi) - 2 \cos(\psi)$ and $\langle W_3 | U^\dagger (-XYY)U | W_3 \rangle = 3 \cos^3(\psi) - \frac{7}{3} \cos(\psi)$ and finally

$$D_{\substack{XXX, -XYY, \\ -YXY, -YYX}}(\text{GHZ}_3 \| U | W_3 \rangle) \\ = -\log \left[\frac{1}{8} (1 + 3z^3 - 2z) (1 + 3z^3 - \frac{7}{3}z)^3 \right], \quad (38)$$

where $z = \cos(\psi)$. This function is minimal at $z = -1/2$.

In conclusion, we found that

$$\mathcal{D}_{S_{\text{GHZ}_3}^*}(\text{GHZ}_3 \| W_3) = \frac{1}{7} \left(-3 \log \frac{5}{6} - \log \frac{13}{16} - 3 \log \frac{43}{48} \right) \\ \approx 0.2235. \quad (39)$$

While our analytical calculation required some symmetry assumptions, this value is also obtained by numerical minimization over all Euler angles.

For the fidelity-based measure \mathcal{F} we note that the rotation we found when minimizing \mathcal{D} gives $|\langle \text{GHZ}_3 | U | W_3 \rangle|^2 = 3/4$. This is known to be the highest possible overlap of the GHZ state with local unitaries (or, indeed, SLOCC) of the W state [27]. With Eq. (24) we obtain

$$\mathcal{F}_{S_{\text{GHZ}_3}^*}(\text{GHZ}_3 \| W_3) = \frac{2}{7}. \quad (40)$$

In Ref. [27] the state

$$|\widehat{W}_3\rangle = \frac{1}{2\sqrt{6}}(3, -1, -1, -1, -1, -1, -1, 3) \quad (41)$$

was found to maximize the overlap of $|\text{GHZ}_3\rangle$ with the SLOCC class of the W state. This state is in fact LU equivalent to $|W_3\rangle$. Though $|\widehat{W}_3\rangle$ minimizes F , it does not minimize D , as it gives the value $D_{S_{\text{GHZ}_3}^*}(\text{GHZ}_3 \| \widehat{W}_3) = -\frac{6}{7} \log \frac{5}{6} \approx 0.2255$.

We want to find families of observables that give the highest values of \mathcal{F} and \mathcal{D} . We claim that any combination of

$$\mathbb{1}ZZ, Z\mathbb{1}Z, ZZ\mathbb{1} \quad (42)$$

is optimal in this sense among all GHZ stabilizing operators. As we have seen above, any element of this family gives $\mathcal{F} = 1/3$ and $\mathcal{D} = -\log(5/6)$. We only have to show that for any other stabilizing operator, or combination of stabilizing operators, there exists a local unitary such that $F \leq 1/3$ and $D \leq -\log(5/6)$. Taking in the above calculations $\cos(\psi) = 1$ we have $\langle W_3 | U^\dagger XXXU | W_3 \rangle =$

1 and $\langle W_3 | U^\dagger (-XYY)U | W_3 \rangle = 2/3$. This proves our claim.

One might ask if these optimal families of observables can be used for the construction of a witness operator for the GHZ entanglement class. This is, however, not the case, as

$$\max_{\text{SLOCC of } W_3} \langle W_3 | (\mathbb{1}ZZ + Z\mathbb{1}Z + ZZ\mathbb{1}) | W_3 \rangle = 3 \quad (43)$$

holds, which can be seen from the fact that the fully separable state $|000\rangle$ gives this value.

We summarize the main results of this subsection:

Observation. *If all GHZ stabilizing operators except the identity are used for the discrimination of the GHZ state from all LU equivalents of the W state, the measures \mathcal{D} and \mathcal{F} are given by Eqs. (39) and (40). If we consider subsets of the stabilizer group, any combination of $\mathbb{1}ZZ$, $Z\mathbb{1}Z$, and $ZZ\mathbb{1}$ is an optimal family of observables, yielding $\mathcal{F} = 1/3$ and $\mathcal{D} = -\log(5/6)$.*

B. Discriminating the W state from the GHZ state

For the reverse problem, the discrimination of $|W_3\rangle$ from the local unitaries of $|\text{GHZ}_3\rangle$, there is no obvious choice of observables, as the W state is not a stabilizer state. However, each of the observables

$$\mathbb{1}\mathbb{1}Z, \mathbb{1}Z\mathbb{1}, Z\mathbb{1}\mathbb{1} \quad (44)$$

has an expectation value of 1/3 for the W state and zero expectation value for all local unitaries of $|\text{GHZ}_3\rangle$, as for the GHZ state all reduced one-qubit density matrices are maximally mixed. Thus any appropriately normalized combination of the above observables gives $\mathcal{F} = 1$, which is the optimal value.

All of these combinations give

$$\mathcal{D}(W_3 \| \text{GHZ}_3) = \frac{2}{3} \log \frac{4}{3} - \frac{1}{3} \log \frac{3}{2} \approx 0.0817. \quad (45)$$

This is the best possible value among all operators occurring in the decomposition of $|W_3\rangle$ in Eq. (37). To see this, we choose the rotation $\varphi = 2\pi/3$, $\theta = 3\pi/2$, and $\psi = 5\pi/4$ on all qubits and observe that all these operators give a value of D less or equal to the one in Eq. (45).

V. GENERAL GRAPH STATES

In the previous sections we observed that the stabilizing operators of a given state are natural candidates for observables that discriminate this state from other states. The graph states are a large class of states which are unambiguously described by their stabilizing operators [22]. In this section we will derive some general statements about the discrimination of graph states.

A graph state is described by its graph, that is, a collection of vertices, each standing for a qubit, and edges

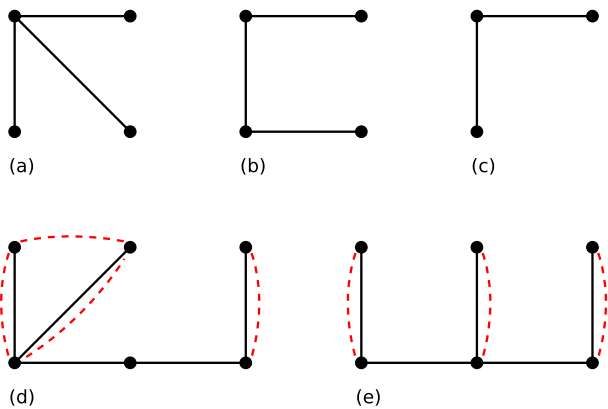


FIG. 3: Graphs of the graph states appearing in the text. (a) Four-qubit GHZ state, (b) four-qubit linear cluster state, (c) three-qubit GHZ state, (d) and (e) the graph states discussed at the end of Section V. In (d) and (e) dashed red lines denote the presence of two-point correlations.

connecting vertices. Some graphs are depicted in Fig. 3. With each vertex (or qubit) i we associate the correlation operator K_i defined as the observable that acts as X on the vertex i and as Z on every vertex in the neighborhood $N(i)$ of i , i. e., all vertices connected to i by an edge

$$K_i = X_i \prod_{j \in N(i)} Z_j. \quad (46)$$

The graph state $|G\rangle$ is defined as the unique common eigenstate of all K_i with eigenvalue $+1$. The products of the K_i form a commutative group S , and the graph state is an eigenstate of all elements of this group. The group S is called the stabilizer group of $|G\rangle$ and its elements the stabilizing operators. For an n -qubit state, that stabilizer group has 2^n elements. The sum of all stabilizing operators $S_i \in S$ gives the projector onto the graph state

$$|G\rangle\langle G| = \frac{1}{2^n} \sum_{i=1}^{2^n} S_i, \quad (47)$$

and Eq. (17) is an example of this general property. The stabilizing operators thus contain a description of all correlations present in the state.

Alternatively from describing perfect correlations, the graph can be understood as a description of the interactions that created the state [22]: Every edge corresponds to an Ising-type interaction and the state is obtained by applying these interactions to the product state $|+\rangle|+\rangle \cdots |+\rangle$. In addition, it should be noted that it is possible for two different graphs to lead to states which are equivalent under local unitary transformations and hence have the same entanglement properties [22].

As an example, we consider the graph in Fig. 3 (a). The generating operators of the stabilizer group are

$$K_1 = XZZZ, K_2 = ZX\mathbb{1}\mathbb{1}, K_3 = Z\mathbb{1}X\mathbb{1}, K_4 = Z\mathbb{1}\mathbb{1}X. \quad (48)$$

After a local change of bases we recognize the graph state as the four-qubit GHZ state with the complete stabilizer group given in Eq. (16). The four-qubit linear cluster state and the three-qubit GHZ state are given by the graphs in Figs. 3 (b) and 3 (c).

In our discussion on the discrimination of the GHZ from the cluster state we learned that the optimal families of observables consist of two-point stabilizing operators. The reason for their optimality is that the cluster state has fewer two-point stabilizing operators than the GHZ state. Hence one may try to derive general results depending only on the numbers of two-point (or higher-order) stabilizing operators.

The number of two-point correlations of a graph state can easily be obtained from its graph [10, 28]. Restricting ourselves to connected graphs with three or more vertices, there are three possibilities to obtain two-point stabilizing operators:

1. Vertices connected to the rest of the graph by only one edge. The generator associated to such a vertex is a two-point operator of the form XZ .
2. Pairs of unconnected vertices whose neighborhoods are equal: $N(i) = N(j)$. The product of the two generators associated to such a pair has the form XX .
3. Pairs of connected vertices for which $N(i) \cup \{i\} = N(j) \cup \{j\}$. This means that their neighborhoods apart from i and j are the same. The product of their generators has the form YY .

The product of the generators associated to vertices i and j is never equal to the identity at positions i and j . Therefore it is a two-point stabilizing operator if and only if it is equal to the identity at all other positions, which leaves only the possibilities 2 and 3. For the same reason the product of three or more generators is never a two-point stabilizing operator. This shows that the above list exhausts all possibilities to obtain a two-point stabilizing operator.

Now, let $|G_1\rangle$ and $|G_2\rangle$ be two graph states, k_1 and k_2 the numbers of two-point correlations of these states, and let P_{G_1} be the set of two-point stabilizing operators of $|G_1\rangle$. We assume $k_1 > k_2$ (our result will be trivial otherwise). We can then derive a lower bound on $\mathcal{F}_{P_{G_1}}(G_1\|G_2)$ and $\mathcal{D}_{P_{G_1}}(G_1\|G_2)$ that depends only on the numbers k_1 and k_2 . Namely, we have

$$\mathcal{F}_{P_{G_1}}(G_1\|G_2) \geq \frac{k_1 - k_2}{k_1}, \quad (49)$$

$$\mathcal{D}_{P_{G_1}}(G_1\|G_2) \geq \frac{k_1 - k_2}{k_1}. \quad (50)$$

To see this, note that from the above discussion it is clear that all two-point stabilizing operators of the same graph state act on different pairs of qubits [28]. It follows that any two-point stabilizing operator of $|G_2\rangle$ can have nonzero overlap with at most one stabilizing operator of

$|G_1\rangle$. This shows that at least $k_1 - k_2$ two-point stabilizing operators of $|G_1\rangle$ will have zero overlap with $|G_2\rangle$, and thus give $\mathcal{F} = \mathcal{D} = 1$. Note that this still holds if local unitaries and permutations of qubits are considered.

For $|G_1\rangle = |\text{GHZ}_4\rangle$ and $|G_2\rangle = |\text{C}_4\rangle$ the bounds give the exact results. This is, however, not always the case, as the example of Figs. 3 (d) and 3 (e) shows: Here, $k_1 = 4$ and $k_2 = 3$. Of the two-point correlations of $|G_1\rangle$, three connect three qubits in a triangle, while for $|G_2\rangle$ the connected pairs are all disjoint. This shows that at most two of the two-point stabilizing operators of $|G_1\rangle$ can have nonzero overlap with $|G_2\rangle$. In this example, $\mathcal{F}_{P_{G_1}}(G_1||G_2) = \mathcal{D}_{P_{G_1}}(G_1||G_2) = 1/2 > 1/4 = (k_1 - k_2)/k_1$.

While one can also use higher-order stabilizing operators for the discrimination, it is more difficult to derive general results for them. Nevertheless, for two given graph states the number of three-point (or higher-order) correlations can directly be computed by writing down the whole stabilizer group; one may then compare the different numbers of higher order stabilizing operators.

VI. DISCUSSION AND CONCLUSION

In this article, we have developed strategies for showing that an experimentally prepared state is not in a certain class of undesired states, given by all local unitaries, or all local unitaries and permutations of qubits, of another state.

We introduced two measures for the discrimination strength of observables. The first measure, denoted by \mathcal{F} , was based on the difference of the expectation values of the observable on either state. It could be interpreted as a noise tolerance, similar to the case of witness operators. The other measure, denoted by \mathcal{D} , was defined as the relative entropy of the probability distributions for the measurement outcomes on either state. It gives a quantitative answer to the discrimination problem by allowing to compare the likelihood that the experimental data origin from the undesired state with, e. g., the likelihood that a sequence of highly biased coin tosses can be explained by a fair coin. In particular, the measure \mathcal{D} is defined in such a way that a maximization of it corresponds to maximizing the discrimination strength while keeping the total number of measurement runs constant, thus answering the question for the best discrimination with limited experimental resources.

We discussed in detail the discrimination of the four-qubit GHZ state from the four-qubit linear cluster state, and vice versa, using stabilizer observables. We also discussed the three-qubit GHZ state and the W state, thus showing that our method can be generalized to states that are no graph states. Finally, we derived a general result on the discrimination of two graph states with the two-point stabilizing operators of one of them, using the power of the graph formalism.

For a specific example we studied the noise tolerance

of the quantities \mathcal{F} and \mathcal{D} and their performance for experimental data. Concerning the comparison of the two measures, our observation that the measure \mathcal{D} is more robust against noise than \mathcal{F} could be explained by the fact that the relative entropy uses all information contained in the probability distributions, while the measure \mathcal{F} effectively reduces each probability distribution to one parameter (namely, the sum of the expectation values). Thus, our conclusion is as follows: Either measure can be used to compare the suitability of different observables for a given discrimination task. For the evaluation of experimental results the relative entropy \mathcal{D} is to be preferred, since it uses all available information and allows for a clear statistical interpretation.

There are several interesting open questions and possible generalizations for the future: First, one could extend our analysis to the measurement of nondichotomic observables or arbitrary product bases [see our discussion of Eq. (27)]. Second, one could consider SLOCC equivalence classes instead of LU classes. Our measures \mathcal{F} and \mathcal{D} are equally applicable for that case, only the optimization is different. Third, one could connect our results to other methods for characterizing multipartite entanglement classes. For instance, there exist witnesses distinguishing the class of mixed three-qubit GHZ states from the class of mixed W states [27]. Here, mixed W states are those three-qubit states that can be written as a mixture of pure states that are biseparable or SLOCC equivalent to the W state. The discrimination of such classes of mixed states is a different problem than the one considered in this article; nevertheless, it would be interesting to understand possible connections.

Acknowledgments

We thank O. Gittsovich, B. Jungnitsch, B. Kraus, E. Solano, and G. Tóth for discussions. This work has been supported by the FWF (START Prize and SFB FOQUS) and the EU (NAMEQUAM, QICS).

Appendix A: Properties of the relative entropy

The relative entropy, also called Kullback-Leibler divergence, from the probability distribution $P = \{p_1, \dots, p_m\}$ to the probability distribution $Q = \{q_1, \dots, q_m\}$ is defined as [18]

$$D(P||Q) = \sum_{i=1}^m p_i \log\left(\frac{p_i}{q_i}\right). \quad (\text{A1})$$

We use the logarithm to the base of two, $\log = \log_2$, and define $0 \log(0) = 0$ (more explicitly: $0 \log(\frac{0}{q}) = 0$, $p \log(\frac{p}{0}) = \infty$, and $0 \log(\frac{0}{0}) = 0$). We list without proof the properties of the relative entropy that are needed in this article:

1. Positive definiteness: $D(P\|Q) \geq 0$ with equality if and only if $P = Q$.
2. $D(P\|Q) = \infty$ if and only if $q_i = 0$, but $p_i > 0$ for some i , that is, if an event is impossible according to the probability distribution Q , but occurs with a nonvanishing probability according to P .
3. $D(P\|Q) \neq D(Q\|P)$ in general, so D is not a metric.
4. Grouping rule: If we decide to consider events 1 and 2 as one event, leaving us with probability distributions $\tilde{P} = \{p_1 + p_2, p_3, \dots, p_m\}$ and $\tilde{Q} = \{q_1 + q_2, q_3, \dots, q_m\}$, then

$$D(P\|Q) = D(\tilde{P}\|\tilde{Q}) + (p_1 + p_2)D(P'\|Q'), \quad (\text{A2})$$

where $P' = \{p_1/(p_1 + p_2), p_2/(p_1 + p_2)\}$ and $Q' = \{q_1/(q_1 + q_2), q_2/(q_1 + q_2)\}$. Note that $D(P'\|Q')$ is the relative entropy within the “box” containing events 1 and 2, and $(p_1 + p_2)$ is the P probability of obtaining an event from this box.

5. If P and Q are the joint probability distributions for two independent random variables, $p_{ij} = p_i^{(1)} p_j^{(2)}$ and $q_{ij} = q_i^{(1)} q_j^{(2)}$, then

$$D(P\|Q) = D(P^{(1)}\|Q^{(1)}) + D(P^{(2)}\|Q^{(2)}). \quad (\text{A3})$$

-
- [1] H. Häffner, C. F. Roos, and R. Blatt, *Phys. Rep.* **469**, 155 (2008).
 - [2] J.-W. Pan, Z.-B. Chen, M. Żukowski, H. Weinfurter, and A. Zeilinger, *Multi-photon entanglement and interferometry* (2008), arXiv:0805.2853.
 - [3] B. Kraus, *Phys. Rev. Lett.* **104**, 020504 (2010).
 - [4] B. Kraus, *Local unitary equivalence and entanglement of multipartite pure states* (2010), arXiv:1005.5295.
 - [5] W. Dür, G. Vidal, and J. I. Cirac, *Phys. Rev. A* **62**, 062314 (2000).
 - [6] F. Verstraete, J. Dehaene, B. De Moor, and H. Verschelde, *Phys. Rev. A* **65**, 052112 (2002).
 - [7] L. Lamata, J. Leon, D. Salgado, and E. Solano, *Phys. Rev. A* **74**, 052336 (2006).
 - [8] T. Bastin, S. Krins, P. Mathonet, M. Godefroid, L. Lamata, and E. Solano, *Phys. Rev. Lett.* **103**, 070503 (2009).
 - [9] M. Van den Nest, A. Miyake, W. Dür, and H. J. Briegel, *Phys. Rev. Lett.* **97**, 150504 (2006).
 - [10] P. Hyllus, O. Gühne, and A. Smerzi, *Phys. Rev. A* **82**, 012337 (2010).
 - [11] O. Gühne and G. Tóth, *Phys. Rep.* **474**, 1 (2009).
 - [12] V. Scarani, A. Acín, E. Schenck, and M. Aspelmeyer, *Phys. Rev. A* **71**, 042325 (2005).
 - [13] N. Kiesel, C. Schmid, U. Weber, G. Tóth, O. Gühne, R. Ursin, and H. Weinfurter, *Phys. Rev. Lett.* **95**, 210502 (2005).
 - [14] C. Schmid, N. Kiesel, W. Laskowski, W. Wieczorek, M. Żukowski, and H. Weinfurter, *Phys. Rev. Lett.* **100**, 200407 (2008).
 - [15] W. van Dam, R. D. Gill, and P. D. Grünwald, *IEEE Trans. Inf. Theory* **51**, 2812 (2005), arXiv:quant-ph/0307125.
 - [16] J. B. Altepeter, E. R. Jeffrey, P. G. Kwiat, S. Tanzilli, N. Gisin, and A. Acín, *Phys. Rev. Lett.* **95**, 033601 (2005).
 - [17] B. Jungnitsch, S. Niekamp, M. Kleinmann, O. Gühne, H. Lu, W.-B. Gao, Y.-A. Chen, Z.-B. Chen, and J.-W. Pan, *Phys. Rev. Lett.* **104**, 210401 (2010).
 - [18] T. M. Cover and J. A. Thomas, *Elements of Information Theory* (Wiley-Interscience, New York, 1991).
 - [19] V. Vedral, *Rev. Mod. Phys.* **74**, 197 (2002).
 - [20] A. Chefles, *Contemp. Phys.* **41**, 401 (2000).
 - [21] Y. Tanaka, D. Markham, and M. Muraio, *J. Mod. Opt.* **54**, 2259 (2007).
 - [22] M. Hein, W. Dür, J. Eisert, R. Raussendorf, M. Van den Nest, and H. J. Briegel, in *Quantum Computers, Algorithms and Chaos*, edited by G. Casati, D. L. Shepelyansky, P. Zoller, and G. Benenti (IOS Press, Amsterdam, 2006), no. 162 in Proceedings of the International School of Physics Enrico Fermi, p. 115, arXiv:quant-ph/0602096.
 - [23] D. Markham, A. Miyake, and S. Virmani, *New J. Phys.* **9**, 194 (2007).
 - [24] S. L. Braunstein, C. M. Caves, R. Jozsa, N. Linden, S. Popescu, and R. Schack, *Phys. Rev. Lett.* **83**, 1054 (1999).
 - [25] W. Wieczorek, C. Schmid, N. Kiesel, R. Pohlner, O. Gühne, and H. Weinfurter, *Phys. Rev. Lett.* **101**, 010503 (2008).
 - [26] P. Badziąg, C. Brukner, W. Laskowski, T. Paterek, and M. Żukowski, *Phys. Rev. Lett.* **100**, 140403 (2008).
 - [27] A. Acín, D. Bruß, M. Lewenstein, and A. Sanpera, *Phys. Rev. Lett.* **87**, 040401 (2001).
 - [28] O. Gittsovich, P. Hyllus, and O. Gühne, *Multiparticle covariance matrices and the impossibility of detecting graph state entanglement with two-particle correlations* (2010), arXiv:1006.1594.